Applied Catalysis B: Environmental 183 (2016) 377–385

Contents lists available at ScienceDirect

Applied Catalysis B: Environmental

journal homepage: www.elsevier.com/locate/apcatb

# Multivariate analysis of the effect of biodiesel-derived contaminants on $V_2O_5$-$WO_3$/$TiO_2$ SCR catalysts

Sandra Dahlin[a], Marita Nilsson[b], Daniel Bäckström[b], Susanna Liljegren Bergman[c], Emelie Bengtsson[d], Steven L. Bernasek[c], Lars J. Pettersson[a,e,*]

[a] Chemical Engineering and Technology, KTH Royal Institute of Technology, SE-100 44 Stockholm, Sweden
[b] Materials Technology, Engine Performance and Emissions, Scania CV AB, SE-151 87 Södertälje, Sweden
[c] Department of Chemistry, Princeton University, Princeton, NJ 08544, United States
[d] SP–Technical Research Institute of Sweden, SE-501 15 Borås, Sweden
[e] Stellenbosch Institute for Advanced Study (STIAS), Wallenberg Research Centre at Stellenbosch University, Stellenbosch 7600, South Africa

ARTICLE INFO

*Article history:*
Received 17 July 2015
Received in revised form
27 September 2015
Accepted 21 October 2015
Available online 27 October 2015

*Keywords:*
$NH_3$-SCR
$V_2O_5$-$WO_3$/$TiO_2$
Chemical deactivation
Design of experiments (DoE)

ABSTRACT

This study investigates the effect of biodiesel-derived contaminants on vanadia-based $NH_3$-SCR catalysts in heavy-duty exhaust aftertreatment. The aim was to study, not only the effect of single contaminants on the catalyst performance, but also of possible interaction effects between poisons.

The effect of six potential catalyst poisons (Na, K, Mg, P, S and Zn) was evaluated using an experimental design and multivariate data analysis. Monolithic $V_2O_5$-$WO_3$/$TiO_2$ catalysts were subjected to accelerated laboratory-scale aging, where the six contaminants were fed simultaneously using a wet impregnation method. In addition to $NO_x$ conversion tests, the catalysts were characterized by means of ICP-OES, SEM-EDX, XPS, $N_2$ physisorption and $NH_3$-TPD. The lab-aged samples were compared to fresh and vehicle-aged catalysts.

The accelerated aging method showed good reproducibility and gave rise to surface compounds similar to those found in vehicle-aged catalysts. Despite plausible differences regarding penetration depth of the contaminants into the walls of the catalyst, the aging method appears to be an efficient way to point out significant chemical poisons.

The model obtained from the experimental design was found to correlate well with the experimental data and can therefore be used to predict effects of the various poisons and poison interactions. Significant effects on the $NO_x$ conversion were found for P, S, Na, Mg and K as well as for the interactions P × Na, P × K and S × Na. A poisoning effect was found for Mg, Na, K, P × K, and P × Na, where Na and K exhibited the strongest poisoning effect. The deactivating effect of alkali was lowered in the presence of phosphorus and sulfur, which is explained by the formation of phosphates and sulfates, preventing the interaction of the alkali metals with the vanadia active sites.



## 1. Introduction

Euro VI emission levels for heavy duty trucks are typically achieved by combining a diesel oxidation catalyst (DOC), a diesel particulate filter (DPF), a selective catalytic reduction (SCR) catalyst and an ammonia slip catalyst (ASC). As the use of alternative fuels in the transport sector grows, a key challenge in exhaust aftertreatment is obtaining a robust system that can handle a variety of fuels and fuel mixtures, while maintaining long-term durability (7 years or 700,000 km for Euro VI) [1].

The catalyst durability is affected by thermal and chemical aging, the latter being caused by components originating from the lube oil and from the fuel. Additives in engine oil, which typically affect the catalyst include Ca, Mg, P, Zn and S. With the introduction of alternative fuels like biodiesel, the exhaust is likely to contain increased levels of P, originating from phospholipids in plants used for production, as well as alkali metals (Na or K) [2,3] or Zn [3] from catalysts used during production of the fuel. Also, alkaline earth metals like Mg and Ca are possible contaminants in biodiesel, resulting from hard water or drying agents used for washing during production [4]. Furthermore, the lower operating temperature of biodiesel compared to fossil diesel fuel increases the risk of more

* Corresponding author at: Chemical Engineering and Technology, KTH Royal Institute of Technology, Stockholm, SE-100 44, Sweden.
*E-mail address:* lpet@kth.se (L.J. Pettersson).

http://dx.doi.org/10.1016/j.apcatb.2015.10.045
0926-3373/

sulfur being accumulated on the catalyst. In summary, P, Na, K, Ca, Mg, Zn and S are potential catalyst poisons during biodiesel operation. These species may reduce the accessible catalytically active surface area, either by adsorbing strongly to the catalyst surface, thereby competing with the reactants in the exhaust, or making active sites inaccessible to the reactants by fouling and pore blocking. A change in electronic or geometric structure of the active sites could also be induced [5].

The focus in this paper is on chemical aging of vanadia-based SCR catalysts. Previous research has shown strong poisoning effects of especially alkali metals [2,6–23], but also alkaline earth metals [2,6–8,11,12], and phosphorus [2,6,7,12,24,25]. Sulfur, on the other hand, has been seen to have a slightly promoting effect [12,23,26]. The major part of the studies is focused on stationary applications [10–22,24,25,27,28] and only a few on mobile applications [2,6,7,9]. Catalysts aged in stationary applications are likely to contain other types of inorganic components at the surface if compared to mobile applications. Furthermore, common to most previous studies is that they cover contamination effects of single contaminants [2,7–9,11–13,17,18,20,24,25]. In some cases, the combined effect of two contaminants present simultaneously have been studied [2,7,8,27]. Very few studies have been performed dealing with cumulative poisoning effects. Klimczak et al. [6] have investigated the effect of single poisons as well as multicomponent systems for screening of cumulative effects using a high-throughput approach for $V_2O_5$-$WO_3$/$TiO_2$ catalysts. The poisoning was found to be related to the basicity of the contaminants and decreased in the order K > Na > Ca > Mg. Synergistic effects were shown for Ca with P and S, respectively, preventing the interaction of Ca with active sites of the catalyst, hence reducing the deactivating effect of calcium. Interaction effects between sulfur dioxide and Na, K, and Ca were also studied in a statistical approach by Guo [23], who found that sulfation together with Na or K resulted in considerably lower deactivation than for Na or K alone.

In real-world aging, the contaminants will rarely be present on the catalyst one at a time. Hence, there is a need for studying the overall effect that relevant contaminants have on the lifetime of the catalyst, as well as evaluating the potential interaction effects between the various poisons. Optimizing experimental conditions and responses by varying one parameter at a time is straightforward, but will not give information about synergistic effects between parameters. The end result will therefore often fail at predicting the true relationship between parameters and the effect they pose on the performance. To overcome this limitation, the experiments can be conducted according to an experimental design, where the parameter values are changed simultaneously. The science of fulfilling demands by changing parameters is called Design of Experiments (DoE), and was first described in 1935 by Sir Ronald Aylmer Fisher.

In this work, the overall effect of six biodiesel-derived catalyst poisons (Na, K, Mg, P, S and Zn) on an $NH_3$-SCR catalyst, aimed for Euro VI heavy-duty applications, has been screened using an experimental design and multivariate data analysis. Monolithic catalyst samples, consisting of $V_2O_5$-$WO_3$/$TiO_2$, were subjected to an accelerated lab-scale aging method, with the simultaneous presence of the six different contaminants. The main purpose of the study was to find which contaminants have the largest impact on the SCR activity and to determine if there are any significant interaction effects between the different poisons. The lab-aged catalyst samples were tested and characterized, and the results were correlated with results from vehicle-aged catalysts.

**Table 1**
Catalyst samples.

| Catalyst ID | Description |
|---|---|
| Fresh (#1–2) | Fresh catalyst samples from two different monolith bricks |
| Lab-aged (#1–38) | Lab-aged catalyst samples |
| Vehicle-aged EU V | Catalyst samples from 250 hp Euro V[1] field test truck, mileage: 130,000 km, long-haulage, Brazil |
| Vehicle-aged EU VI | Catalyst samples from 480 hp Euro VI[2] FAME field test truck, mileage: 700,000 km, long-haulage, Germany |

[1]SCR; [2]DOC + DPF + SCR + ASC.

## 2. Experimental

Fig. 1 shows a schematic overview of the experimental procedure, further described in the following sections.

### 2.1. Catalyst samples

For this study, a commercial 260 cpsi $V_2O_5$-$WO_3$/$TiO_2$ SCR catalyst from Haldor Topsøe was used. The catalyst is based on fiberglass-reinforced titania support material in a corrugated shape. Cylindrical samples with a diameter of 25 mm and a length of 45 mm were drilled out from two different fresh monoliths. 38 samples were used for the lab-aging. All samples were degreened in a muffle furnace for 5 h at 450 °C in air, in order to achieve a stable activity of the catalyst. Fresh, lab-aged and vehicle-aged catalyst samples are hereafter denoted as shown in Table 1.

### 2.2. Catalyst activity measurements

The catalyst activity measurements were performed in a lab-scale tubular quartz reactor operating at atmospheric pressure. The activity for $NH_3$-SCR Eq. (1) was measured at 375, 300 and 250 °C, respectively, with an inlet gas mixture comprising 8 vol% $O_2$, 0.1 vol% NO, 0.1 vol% $NO_2$, 0.2 vol% $NH_3$, 6.5 vol% $H_2O$ and balance $N_2$ ($GHSV_{NTP}$ = 50,000 $h^{-1}$). An Eco Physics CLD 822 chemiluminescence detector was used for analysis of the $NO_x$ concentration in the gas. The $NH_3$ concentration was measured with an FTIR instrument (BOMEM, Hartmann & Braun, MB-100).

$$NO + NO_2 + 2NH_3 \rightarrow 2N_2 + 3H_2O \quad (1)$$

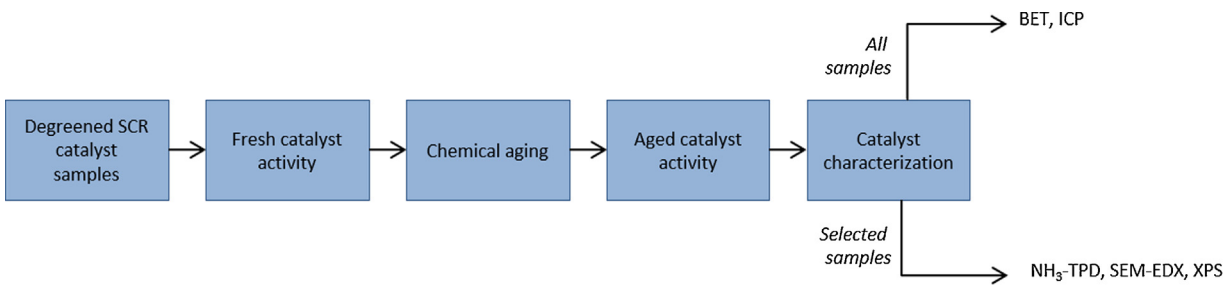


**Fig. 1.** Experimental procedure.

The catalyst activity was evaluated based on the conversion of $NO_x$ according to Eq. (2).

$$\%NO_x\text{conversion} = \left(1 - \frac{[NO_x]_{out}}{[NO_x]_{in}}\right) \times 100 \quad (2)$$

Activity measurements were performed for fresh catalyst and following the aging procedure for every sample, as shown in Fig. 1.

### 2.3. Accelerated chemical aging

Contamination of the catalyst samples was performed using a wet impregnation method. The samples were immersed in a contaminating solution containing aqueous salts of the different elements, while applying vacuum in order to remove air bubbles which could otherwise block the channels of the substrate. The contaminating solution was prepared by mixing two stock solutions, one containing dissolved nitrate salts of Zn, Na, Mg and K in purified water, and the other containing a ligand (EDTA) and dissolved ammonium salts of P and S in 5 vol% $NH_3$. The addition of EDTA stabilizes the metal salts for the duration of the contamination procedure, which would otherwise precipitate in the presence of phosphate and sulfate and necessitate a two-step contamination procedure, leading to difficulties achieving reproducible contamination levels. Ammonia was added to increase the solubility of EDTA.

Two levels of contamination were used, targeting 0.25 wt% of each poison for the low level and 1 wt% for the corresponding high level. After the described chemical aging procedure the catalyst samples were dried in two steps, a first step at 105 °C overnight followed by a further drying at 375 °C for 3 h.

### 2.4. Experimental design—screening of poisoning effect

In the present study, the combined effect of six potential catalyst poisons, P, S, Na, K, Zn, and Mg, on the $NH_3$-SCR performance of a vanadia-based SCR catalyst, was studied. An experimental design was constructed aiming at, as a minimum, resolving main effects of each contaminant as well as interaction effects for P and S. The chosen design was in the form of a $2^{6-1}$ reduced factorial design, which is based on two concentration levels (one high and one low level, as previously described) for each of the six contaminants. This type of design is also commonly known as a screening design. After the inclusion of 6 replicates, the chosen design resulted in totally 38 (32 + 6) observations. The main purpose of the design was to find which contaminants have an important impact on the $NH_3$-SCR activity and to reveal important interaction effects between the contaminants. This means that, in the design, the activity of the catalyst is analyzed with respect to the concentrations of contaminants in the sample.

The results were evaluated using Multiple Linear Regression (MLR) [29]. MLR models the linear relationship between the independent variables ($X$) and the responses ($Y$):

$$Y = X\beta + \epsilon$$

where $Y$ is the response vector or matrix (i.e., for one or multiple responses, respectively), $\beta$ is the regression matrix containing the regression coefficients, and $\epsilon$ is the error, or residual, matrix. The matrix $X$ contains all the design parameters taken from the reduced factorial design, both the main factors and the interactions of interest. In this study, the response vector $Y$ represents the $NO_x$ conversion of the contaminated samples and $X$ represents the poison concentrations according to the experimental design (the actual measured concentration of each poison and not the target value, though the actual and target concentrations were rather similar). β is calculated, and represents the coefficients for each poison. The parameter describes the contribution of each variable to the model, i.e., the magnitude of the poisoning effect on the $NO_x$ conversion, relative to the model mean. $\epsilon$ is the non-modeled variance, i.e., residuals. Factors investigated are the main contaminants (P, S, Na, K, Mg, and Zn) and interaction effects between S and P with any other poisons, e.g., P × Na, S × Na, S × P etc.

Prior to analysis, all $X$ variables (factors) where centered and scaled to Unit Variance (UV), a procedure also known as autoscaling. That means for each variable, the mean value and standard deviation is calculated. The mean is then subtracted from the data and the remainder is divided by the standard deviation. This is done to negate the effect of larger values contributing more to the model than smaller values. By the use of analysis of variance (ANOVA), we can for each effect (main factors and interactions) calculate the probability that they explain more of the variation in the response variable than what could be expected from random phenomena. Only factors and interactions with a $p$ value lower than 0.05 (i.e., 95% confidence or higher), are used in the final model.

### 2.5. Catalyst characterization

#### 2.5.1. Bulk elemental analysis—ICP-OES

Inductively coupled plasma optical emission spectroscopy (ICP-OES) was used to measure the actual bulk concentration of contaminants of all the catalyst samples. The technique was also applied for measuring the V and W content of the samples to validate that the aging procedure did not cause leaching of active material from the catalyst samples. The samples were prepared by grinding followed by digestion in $HNO_3$ + HCl + HF in a laboratory microwave oven prior to the analysis in an Optima 8300 PerkinElmer instrument.

#### 2.5.2. Specific surface area—$N_2$ physisorption

The BET surface area of fresh as well as lab- and engine-aged samples was measured by nitrogen physisorption at −196 °C in a Micromeritics Tristar 3000 instrument. The samples were analyzed with 5 points in the interval $P/P_0 = 0.05 - 0.3$. Prior to the measurements, the catalysts were degassed at 150 °C for 4 h.

The BET surface areas for the lab-aged samples were included as a parameter in the experimental design used for the activity measurements. The purpose was to investigate if there are any significant correlations between chemical contamination and surface

**Table 2**
Comparison of concentration of contaminants in the bulk for fresh, lab- and vehicle-aged samples. Presented as at% ratio.

| | Sample | | | | | |
|---|---|---|---|---|---|---|
| | Fresh | Lab-aged #1 | Lab-aged #22 | Lab-aged #37 | Vehicle-aged EU V | Vehicle-aged EU VI |
| Na/V | 0.18 | 2.2 | 1.8 | 2.0 | 0.09 | 0.13 |
| K/V | 0.09 | 1.3 | 1.1 | 1.3 | 0.08 | 0.09 |
| Mg/V | 0.17 | 1.7 | 1.6 | 0.58 | 0.29 | 0.14 |
| P/V | 0.26 | 1.4 | 1.4 | 1.5 | 0.48 | 0.33 |
| S/V | 0.05 | 1.3 | 1.4 | 0.36 | 0.22 | 0.21 |
| Zn/V | <0.01 | 0.61 | 0.12 | 0.12 | <0.01 | <0.01 |

area on the SCR catalyst activity and to investigate the effect of the different contaminants, and their interactions, on the surface area of the catalyst.

*2.5.3. Acidity—$NH_3$-TPD*

The surface acidity of a subset of the lab-aged samples from the experimental design, as well as fresh and vehicle-aged samples, was determined in a Micromeritics TPD/TPR 2900 analyzer with an in-situ pretreatment and successive $NH_3$-TPD analysis. In the TPD analyzer, the sample was subjected to a temperature program from room temperature up to 450 °C in helium, using a ramp rate of 10 °C/min. The sample then remained at 450 °C for 30 min in flowing helium. After cooling down in helium to 50 °C, the sample was alternately flushed with ammonia for 10 min and with helium for 10 min. This procedure was repeated 3 times. The temperature was then raised to 150 °C using a ramp rate of 5 °C/min and held constant until a stable baseline was obtained. Finally, desorption of ammonia was monitored in the temperature range of 150–450 °C (ramp rate 10 °C/min). The dry sample weight, obtained by weighing the sample after the analysis, was used in the calculations of the specific acidity.

*2.5.4. Surface elemental analysis—XPS*

X-ray photoelectron spectroscopy (XPS) was used to evaluate the surface composition and oxidation states of the elements of lab-aged as well as fresh and vehicle-aged catalyst samples. The XPS experiments were carried out with a VG ESCA Lab Mk.II instrument, using Mg Kα (1253.6 eV) emission at a pass energy of 20 eV. The instrument has a two-point calibration to the Au $4f_{7/2}$ (84.0 eV) and Cu $2p_{3/2}$ (932.7 eV) peaks. Individual samples are calibrated to the C 1s position. Peaks are fitted using the CASA XPS software and a Shirley background. Standard values for area/position constraints as well as relative intensities of spin orbit components were employed. The resolution of the instrument enables peaks to be resolved within 0.5 eV of each other.

*2.5.5. Elemental mapping of contaminants—SEM-EDX*

SEM images were obtained on a Carl Zeiss FE-SEM (Sigma VP) electron microscope using a variable pressure secondary electron detector. Elemental mapping was performed by energy-dispersive X-ray spectroscopy (EDX) using an X-Max 50 detector from Oxford Instruments.

## 3. Results and discussion

### 3.1. Accelerated chemical aging

The accelerated chemical aging method was evaluated by means of ICP-OES, SEM-EDX and XPS. ICP-OES analyses of the different contaminants verified that the levels of contamination, high and low respectively, were in good agreement with the target concentrations and that the variation within each level was low, see Fig. 2. It was also confirmed that the contamination procedure did not cause loss of active V or W from the catalyst samples.

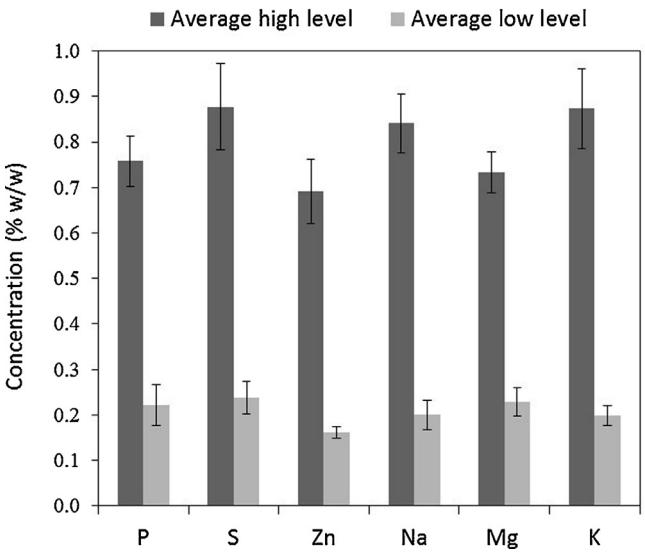


**Fig. 2.** Measured concentrations of contaminants in the lab-aged samples. Target levels were 0.25 and 1 wt% for the high and low level, respectively. The error bars correspond to ± one standard deviation.

Table 2 shows results from elemental analysis of the contaminants in the bulk for fresh, lab-aged and vehicle-aged catalysts. Two vehicle-aged catalysts were included in the study, one from a Euro V vehicle, equipped with SCR catalyst only, the other from a Euro VI system, where the catalyst was located downstream an oxidation catalyst and a particulate filter. In addition to the fact that the SCR catalyst is positioned downstream the DOC and DPF, meaning that it is exposed to already treated exhaust, it generally appears robust towards chemical poisoning. Both vehicle-aged catalysts studied contained elevated, but not remarkably high, amounts of sulfur. It is not surprising to detect sulfur in downstream components, as it is a reversible poison and therefore can be released from DOC and DPF during high-temperature operation. Irreversible poisons will put higher strains on upstream components. The Euro V catalyst additionally contained slightly higher amounts of phosphorus compared to the fresh catalysts. The amount of poisons in the vehicle-aged catalysts is overall considerably lower compared to the lab-aged catalysts. The higher concentrations during lab-aging were preferred in order to obtain large effects on the performance and thereby more significant results, although still within the region of linear response. Elemental mapping by SEM-EDX of the catalyst wall cross sections was used to study the distribu-

**Table 3**
Results of XPS measurements of fresh- lab- and vehicle-aged samples. Binding energies (eV) and following assignment of the peaks to probable elements. A difference in binding energy of 0.5 eV can be considered significant.

| | Sample | | | | |
|---|---|---|---|---|---|
| | Fresh | Lab-aged #1 | Lab-aged #22 | Lab-aged #37 | Vehicle-aged EU VI |
| K 2p | nd | 293.6[1] | 293.5[1] | 293.2[1] | nd |
| Na 1s | nd | 1071.7[2] | 1071.9[2] | 1071.9[2] | 1071.7[2] |
| Zn 2p | nd | 1022.4[3] | 1022.4[3] | nd | nd |
| W 4f | 35.7[4] | 35.7[4] | 35.5[4] | 35.8[4] | 35.5[4] |
| S 2p | nd | 169.7[5] | 169.7[5] | nd | 169.7[5] |
| P 2p | 133.4[6] | 133.4[6] | 133.6[6] | 134.1[6] | 133.6[6] |
| O 1s + | 531.3[7] and 532.8[8] | 530[7] and 532.4[8] | 530.1[7] and 532.7[8] | 530.4[7] and 533.2[8] | 530[7] and 532.9[8] |
| V 2p | around 516[a,9] | nd | 516.8[9] | nd | 516.8[9] |

[a]Difficult fit; nd – not detected. [1]$K_3PO_4$, [2]$Na_2SO_4$ or $Na_4P_2O_7$, [3]ZnO, [4]$WO_3$, [5]$SO_4^{2-}$, [6]$PO_4^{3-}$ or $PO_3^-$, [7]metal oxide, [8]hydroxide, [9]oxide.

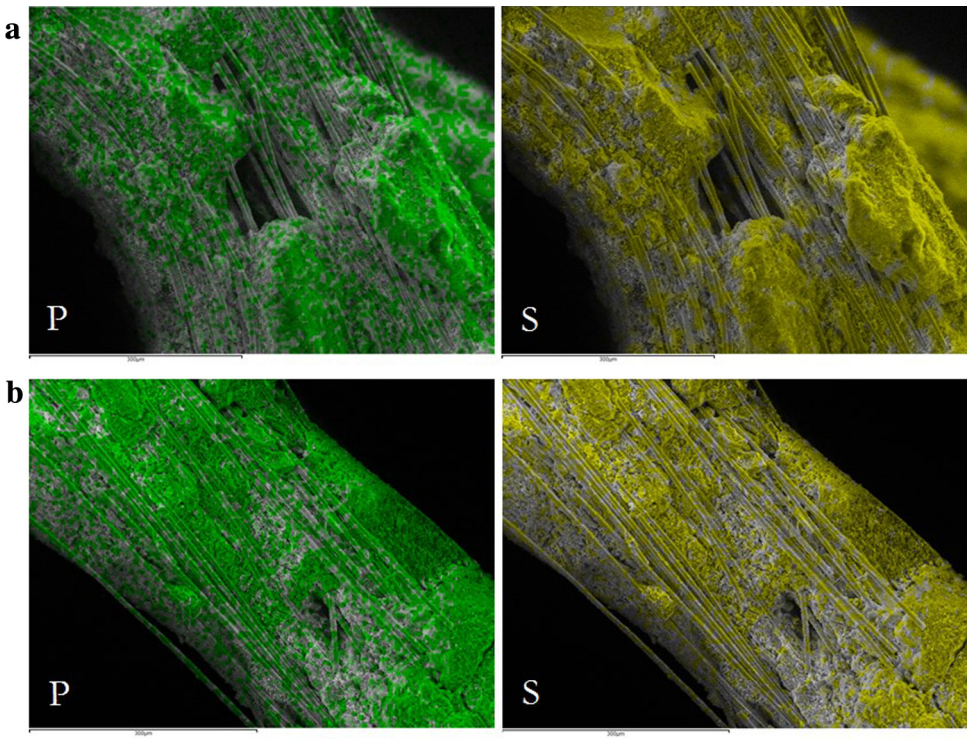


**Fig. 3.** Elemental mapping by SEM-EDX comparing the distribution of phosphorus (green) and sulfur (yellow) in a (a) vehicle-aged and (b) lab-aged catalyst.
(a) Vehicle-aged EU V.
(b) Lab-aged #22 (High Na, Mg, P, S, K).

tion of poisons in the lab-aged samples and to identify possible differences with respect to the vehicle-aged catalysts. By studying the elemental maps of the lab-aged catalysts, it was found that all contaminants were homogeneously distributed throughout the walls of the catalyst. The wet impregnation method used in this study results in a complete wetting of the catalyst. This is likely to cause differences compared to aging in real exhaust, something that, however, could not be detected by SEM-EDX. Both phosphorus and sulfur were relatively uniformly accumulated in the catalyst material of the vehicle-aged catalysts, see Fig. 3. Nevertheless, the difference in aging methodology needs to be considered during evaluation of the results. Aging by aerosols is an alternative to wet impregnation for accelerating deactivation. Results from the literature is contradictory when it comes to which method that gives rise to the most deactivating effect. Larsson et al. [18] found that impregnation had a larger impact than aerosol aging, while an opposite effect was shown by Klimczak et al. [6] and Castellino et al. [24]. XPS analyses were performed on fresh #1, vehicle-aged EU VI and lab-aged #1, 22 and 37 (see Table 1 for denotations). The lab-aged samples #1 and #22 were evaluated as they contained the highest total amount of contaminants of all aged samples, while #37 was studied as it contained high levels of P, Na and K, which were the contaminants found to be present when the acidity was affected the most (further discussed in Section 3.2.2). Table 3 shows the binding energies of the contaminants detected in each sample. Magnesium could not be analysed, since a magnesium anode was used for data acquisition.

Potassium and zinc were found in lab-aged but not in fresh or vehicle-aged samples. The binding energy of potassium is similar for all samples, 293.2–293.6 eV, and indicates that potassium is in the form of potassium phosphate ($K_3PO_4$). Zinc was found at a binding energy of 1022.4 eV, representing zinc oxide. Previous research suggests formation of zinc oxide or pyrophosphate ($Zn_2P_2O_7$), while the poisoning effect of potassium has been ascribed to strong

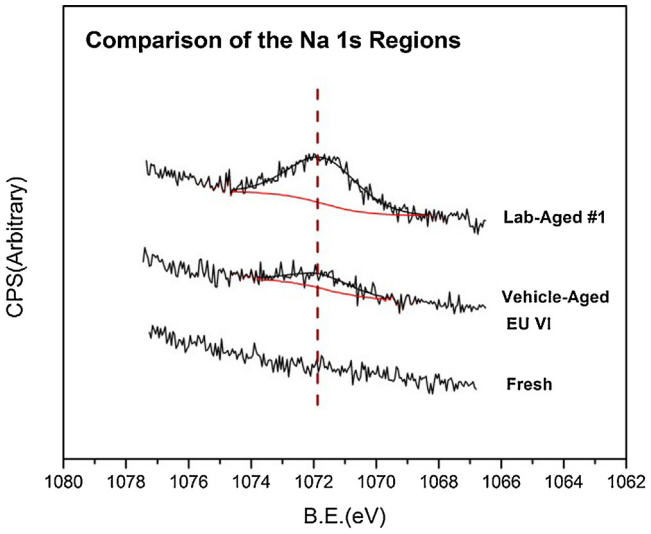


**Fig. 4.** Deconvolution of the Na 1s XPS spectra for a lab-aged sample compared to vehicle-aged and fresh sample. Sodium is present in the form of $Na_2SO4$ or $Na_4P_2O_7$.

interactions with vanadium through the formation of potassium vanadates [2].

Sodium was found in all aged samples, both lab- and vehicle-aged, at similar binding energies of 1071.7–1071.9 eV, see Fig. 4. This corresponds likely to either sodium pyrophosphate ($Na_4P_2O_7$) or sodium sulfate ($Na_2SO_4$). In the fresh samples, no sodium was detected. According to the bulk chemical analysis, the amount of sodium in the vehicle-aged samples was not increased compared to the fresh catalysts, i.e., the sodium is only present at the outer surface. This could, however, not be distinguished by SEM-EDX.

Sulfur was found in lab-aged and vehicle-aged samples, at a binding energy of 169.7 eV, and is hence likely a sulfate. No sulfur

**Table 4**
Surface area and total acidity of lab-aged catalyst samples, expressed as percentage of the value obtained for fresh catalyst.

| Catalyst sample | Relative surface area (% of fresh)[a] | Relative total acidity (% of fresh)[a] | Relative NO conversion[b] (% of fresh) |
|---|---|---|---|
| Lab-aged #1 | 54 | 11 | 65 |
| Lab-aged#14 | 63 | 48 | 89 |
| Lab-aged #16 | 63 | 50 | 99 |
| Lab-aged #19 | 67 | 80 | 98 |
| Lab-aged #22 | 58 | 19 | 81 |
| Lab-aged #24 | 51 | 52 | 97 |
| Lab-aged #27 | 58 | 46 | 96 |
| Lab-aged #37 | 58 | 11 | 63 |
| Vehicle-aged Euro VI | 88 | 84 | 99 |

[a] Relative to the average of two fresh samples.
[b] @ 300 °C.

was detected in the fresh sample. Sulfates are formed when sulfur oxides react with ammonia or interact with the SCR catalyst surface [23]. Sulfates can be formed on the catalyst surface both during aging with $SO_2$ [23,30,31] and $SO_3$ [30]. Sulfation can inhibit NO adsorption in the presence of oxygen, but promote $NH_3$ adsorption on vanadia-based SCR catalysts by increasing the amount of Brønsted acid sites [23].

Phosphorus was detected in all samples at a binding energy in the interval between 133.4 and 134.1 eV, which agrees well with phosphate ($PO_4^{3-}$) or metaphosphate ($PO_3^-$). The fresh catalyst showed a phosphorus peak at the same binding energy as the aged samples. Both phosphate, metaphosphate as well as phosphorus pentoxide ($P_2O_5$) have been reported in previous studies of SCR catalyst aging [32,33].

Vanadium was difficult to detect by XPS. This could be a result of contaminants covering the vanadium, hence making it hard to detect by a surface sensitive technique, or due to overlap with other peaks present in the oxygen region. Phosphorus has previously been shown to cover the catalyst surface to such an extent that the peak related to vanadium in XPS vanished [6]. In the samples where vanadium was detected, and a good peak fit was possible, the binding energy was 516.6–516.8 eV. While this binding energy corresponds to vanadium oxide, it is not possible to specify the oxidation state, as the binding energies of different oxidation states for vanadium ($V^{3+}$, $V^{4+}$, and $V^{5+}$) are within around 0.5 eV of each other [34].

Tungsten was easily detected in all samples at a binding energy of 35.5–35.8 eV, which is consistent with an oxide. No differences were observed between fresh, lab-aged and vehicle-aged samples. This is in agreement with previous studies on chemically aged $V_2O_5$-$WO_3$/$TiO_2$ catalysts, where no change in the V 2p, W 2p or Ti 2p XPS peaks has been observed [25].

Two peaks related to oxygen were found in all samples. The first peak, at a binding energy of around 530–531 eV, is related to a metal oxide, e.g., oxygen binding to titanium, vanadium or tungsten. The other peak, at a binding energy of around 532–533 eV is likely related to surface hydroxyl groups, as previously assigned by other authors [8,11]. The binding energy of the peak related to the metal oxide differs about 1 eV between aged (lab- and vehicle-aged) and fresh samples, the former between 530.0–530.4 eV and the latter at 531.3 eV. This difference could be explained by partial incorporation of hydroxyl groups in the metal oxide matrix as the sample ages at high temperature. As the overall electron density changes, the peak shifts to a lower binding energy and broadens, corresponding to an average increase in the oxidation states present. Previous work by Chen et al. [11] supports changes in the oxygen region upon aging $V_2O_5$-$WO_3$/$TiO_2$ SCR catalysts with alkali metals.

In summary, even if the wet impregnation aging results in a complete wetting of the catalyst, and therefore not precisely simulates real-world chemical aging effects, it is considered to be a useful tool to evaluate the significance of the various poisons and their possible interaction effects. The surface compounds of at least phosphorus, sodium and sulfur were similar in the lab- and vehicle-aged catalysts, as shown by XPS. Potassium and zinc were not found at the surface of the vehicle-aged samples and, therefore, no conclusion could be drawn regarding those surface compounds.

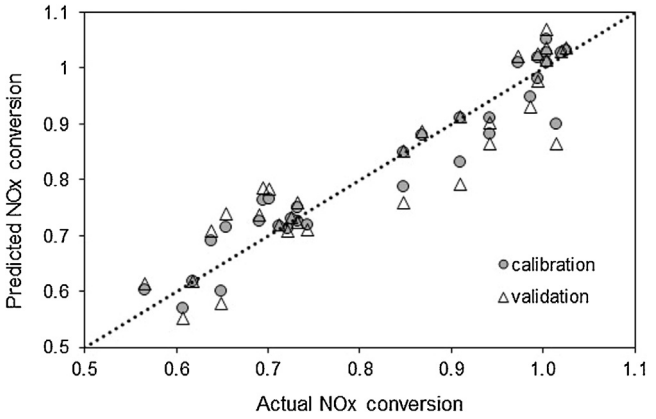


**Fig. 5.** Predicted versus actual relative $NO_x$ conversion @ 375 °C for the contaminated catalyst samples. Circles and triangles represent calibration (model with all data points included, $R^2 = 0.92$) and validation (cross-validated, $R^2 = 0.85$) values, respectively.

## 3.2. Evaluation of the experimental design

### 3.2.1. $NH_3$-SCR activity—evaluation of poisoning effect

The $NO_x$ conversion of the fresh catalysts was around 75, 98, and 96 % for the temperatures 250, 300, and 375 °C respectively. The variation in activity between the fresh samples was low, <1.5 % RSD. The $NO_x$ conversion of the lab-aged catalyst samples was in the range 54–113 % relative to the activity of the corresponding fresh catalyst, i.e., contamination did not consistently result in significant changes in catalyst activity. The replicates displayed good agreements, 1 % relative standard deviation (RSD).

The result from evaluation of the experimental design is shown in Figs. 5 and 6. Fig. 5 shows that the obtained model for the $NO_x$ conversion expresses a good correlation with the experimental data and can therefore be used to predict the effects of various poisons and poison interactions. Fig. 6 shows the β-coefficients obtained for the main poisons and poison interactions, i.e., the influence of the various factors on the $NO_x$ conversion. Only the factors that were significant at a 95% confidence level are included in the figure. There was no obvious difference in behaviour between different temperatures other than a more pronounced pattern (higher signal-to-noise ratio) at higher temperatures.

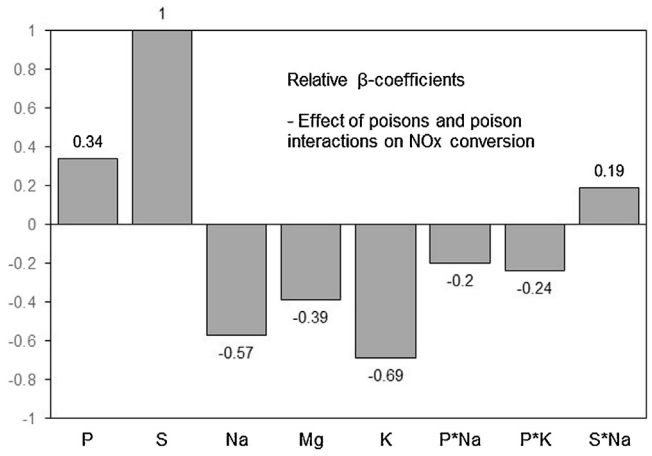


**Fig. 6.** Centered and scaled β-coefficients for all poisons and poison interactions that were significant on a 95 % confidence level. Negative values correspond to a more negative effect on $NO_x$ conversion than the model mean, while positive values correspond to a less negative effect than the model mean.

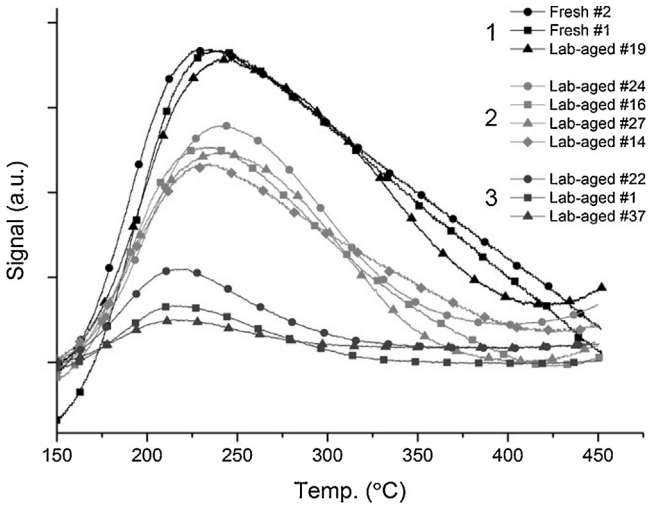


**Fig. 7.** $NH_3$-TPD profiles of fresh and lab-aged samples. The three levels, numbered 1, 2 and 3, respectively, are further compared in Table 5. Level 1 corresponds to the profiles with $NH_3$ uptakes similar to fresh catalyst and level 3 to the profiles with the largest effect on the uptake.

From the results in Fig. 6 it can be concluded that the following factors (i.e., contaminants) and two-factor interactions significantly affect the $NO_x$ conversion of the SCR catalyst: P, S, Na, Mg, K, P × Na, P × K and S × Na. Most of the factors, Na, K, Mg, P × K, and P × Na, display a negative effect on the $NO_x$ conversion, i.e., a poisoning effect. The greater the negative value, the more poisoning is the effect, i.e., K and Na are the strongest poisons.

The interaction of P with the alkali metals and of S with Na resulted in a decreased poisoning effect compared to the single effects of Na and K. An explanation for this could be the formation of phosphates and sulfates, which prevents the alkali metals from interacting with active sites. This agrees well with the fact that both sodium and potassium phosphates as well as sodium sulfates were detected at the surface by means of XPS. Furthermore, the model neither showed any significant effect for the interaction of potassium with sulfur, nor were any potassium sulfates found at the surface of the contaminated samples. An effect of phosphate and sulfate formation could also be increased ammonia storage capacity of the catalyst, something that, however, could not be confirmed with the present experimental design.

The single contaminants S and P instead exhibit a positive effect. Note that a positive effect in this case should be interpreted as a reduced poisoning effect with respect to the model mean, and not as an increased activity. This interpretation is based on the fact that the scope of the experimental design does not include zero levels of contaminants, and it is therefore not possible to separate a true positive effect from the effective/apparent result, i.e., a reduced poisoning effect. The same effect was shown for the S × Na interaction, but to a smaller degree. Also noteworthy was that the model did not show any significant effect of Zn on the $NO_x$ conversion.

### 3.2.2. Surface area and acidity

The surface area was measured for all samples, while $NH_3$-TPD was performed on a selection of samples, as described in the experimental section. The surface areas of the selected catalysts are displayed in Table 4, expressed as percentage of fresh catalyst surface area, together with the relative total acidity from $NH_3$-TPD (total $NH_3$-uptake) and the relative $NO_x$ conversion, also compared to the values for the vehicle-aged catalysts.

The surface area of all lab-aged samples were lower compared to the fresh catalysts, ranging between 51 and 67% of the value for the fresh catalysts. Evaluation of the effect of contaminants on the surface area using the experimental design (all 38 samples) results in no clear correlation between surface area and specific contaminants. The model results in an $R^2$ value of only 0.44, with all measuring points included, which is poor. There appears, however, to be a tendency towards a decrease in the surface area for the main factors P and Mg. P is known to deactivate aftertreatment catalysts by coverage of active sites through fouling and pore blocking of the surface, resulting in decreased surface area [6]. Mg is also a known fouling agent during $NH_3$-SCR, especially for stationary applications [35]. This result shows that both chemical and physical mechanisms contribute to the deactivation.

The adsorption of ammonia on the surface is an essential step during $NH_3$-SCR [36,37]. Therefore, the performance is strongly related to the acidity of the catalyst. The total acidity of the lab-aged samples (Table 4) ranges from 11 to 80% compared to fresh catalyst. The $NH_3$-TPD curves are shown in Fig. 7. Ammonia is desorbed over a wide temperature range, showing the presence of both weakly and strongly bound ammonia. Most profiles have not yet returned to the baseline level at the end of the temperature programme, suggesting that these samples still desorb $NH_3$ at 450 °C. For some of the lab-aged samples the acidity is strongly affected, while for others, the effect is not as pronounced. The profiles are separated in three distinct levels, at around 15% (lab-aged #1, 22, 37), 50% (lab-aged #14, 16, 24, 27) and 80% (lab-aged #19) relative total acidity. Also, for the samples with the lowest total acidity, the peak maxima is moved to a slightly lower temperature, indicating that the strength of the acid sites is somewhat reduced. Alkali metal poisoning has previously been ascribed to a decreased amount of Brønsted acid sites as well as decreased reducibility of the active vanadia sites [14].

Comparing the samples within each level in Fig. 7 (see Table 5) reveals that they have similar amount of total contaminant concentration. Furthermore, there appears to be a correlation between alkali metal poisoning and total acid amount. Common to the samples with the lowest ammonia storage capacity is that they have been contaminated with high levels of Na, K as well as P. The subset of 8 samples from the full data set was analysed with respect to surface acidity using the experimental design. As the number of samples was less than the number of variables, multiple linear regression (MLR) was not a viable choice directly (due to an underdetermined system of equations). The variables that were found to correlate most to the TPD-values were therefore determined using Partial Least Squares (PLS) regression. Eliminating all but the two alkali metals (Na and K) resulted in a model with an acceptable

**Table 5**
Comparison of the samples within the three different levels (1, 2 and 3) in Fig. 6 and related to the vehicle-aged catalysts.[a]

| | | | | |
|---|---|---|---|---|
| $NH_3$-uptake similar to fresh | | | | |
| Sample | #19 | | | |
| Relative $NH_3$ uptake (%) | 80 | | | |
| Relative $NO_x$ conversion (%) | 98 | | | |
| Relative surface area (%) | 67 | | | |
| Total poison conc. (wt%) | 2.8 | | | |
| Poisons in high conc. level | Mg, P, S | | | |
| Medium effect on $NH_3$-uptake | | | | |
| Sample | #14 | #16 | #24 | #27 |
| Relative $NH_3$ uptake (%) | 48 | 50 | 52 | 46 |
| Relative $NO_x$ conversion (%) | 89 | 99 | 97 | 96 |
| Relative surface area (%) | 63 | 63 | 51 | 58 |
| Total poison conc. (wt%) | 3.4 | 2.0 | 3.7 | 3.2 |
| Poisons in high conc. level | Na, S, Zn, Mg | P, Zn | P, S, K, Zn | Na, P, S |
| Large effect on $NH_3$-uptake | | | | |
| Sample | #1 | #22 | #37 | |
| Relative $NH_3$ uptake (%) | 11 | 19 | 11 | |
| Relative $NO_x$ conversion (%) | 65 | 81 | 63 | |
| Relative surface area (%) | 54 | 58 | 58 | |
| Total poison conc. (wt%) | 4.8 | 4.0 | 3.1 | |
| Poisons in high conc. level | All | Na, Mg, P, S, K | Na, P, K | |
| Vehicle-aged catalysts | | | | |
| Sample | EU V | EU VI | | |
| Relative $NH_3$ uptake (%) | n.a. | 84 | | |
| Relative $NO_x$ conversion (%) | 98 | 99 | | |
| Relative surface area (%) | 87 | 88 | | |
| Total poison conc. (wt%) | 0.7 | 0.2 | | |
| Poisons in high conc. level | P, S | S | | |

[a] Relative values are normalized with respect to numbers for fresh catalyst.

$Q^2$—value of 0.71 (corresponding to $R^2$ for the validated model, using the standard Leave-One-Out (LOO) cross validating method). Including P did not result in a more robust model.

Correlating total acidity and $NO_x$ conversion is not completely straightforward. The total amount of ammonia adsorbed will decrease with increasing amount of poisons. Ammonia will adsorb on all types of acid sites, but reaction with gaseous NO will only occur if it is adsorbed on vanadia active sites [23,38–40]. Therefore, care has to be taken when correlating the effect of the contamination to the total amount of ammonia adsorbed. The samples that had the highest influence on the ammonia storage capacity also exhibited significantly decreased activity for $NO_x$ conversion. For the group of samples with relative total amount of adsorbed ammonia around 50%, the activity was only slightly influenced ($NO_x$ conversion 89–99 % of fresh) despite the fact that the surface areas had been significantly affected.

The results clearly indicate that the amount of poisons, particularly alkali metals, significantly affects the ammonia adsorption capacity. There is no evident correlation between surface area and acidity. This may be explained by the fact that the various contaminants affect the acidity differently. For example, sulphates could influence the surface area negatively, but the ammonia storage capacity positively. Such effects will make an interpretation of correlations between different characteristics difficult. The surface area is, instead, mainly affected by typical fouling agents, like P and Mg. The ammonia adsorption capacity is shown to be more critical for the $NO_x$ conversion compared to the specific surface area. A 50% decrease in surface area does not considerably affect neither the amount of ammonia adsorbed nor the $NO_x$ conversion.

The results also correlate well with those for the vehicle-aged catalysts, though these catalysts were not as heavily contaminated as the lab-aged samples.

### 3.3. Significance and practical implications of the study

This study has provided a toolbox that can be used to understand the impact of a certain chemical load for SCR catalysts. Deactivation factors can be derived from the developed model, which can be used to quantify the effect of poisons present on a catalyst. The methodology is, together with models describing thermal aging, used to quantify the overall catalyst aging and to predict remaining catalyst lifetime. A successful transition of the findings from the study into real-world conditions will include further studies focussing on fundamental understanding of the deactivation mechanisms during interactions between the significant contaminants. Furthermore, the findings from the study are used as input for optimization and validation of new and more robust catalyst technologies, meeting upcoming challenges with respect to fuel diversity.

## 4. Conclusions

The overall effect of six biodiesel-derived catalyst poisons (Na, K, Mg, P, S and Zn) on a vanadia-based $NH_3$-SCR catalyst has been evaluated using an experimental design and multivariate data analysis. It was shown that wet impregnation poisoning in laboratory scale can be used to study the effect of chemical catalyst poisoning in a repeatable as well as time- and cost-efficient way. Surface compounds of phosphorus, sodium and sulfur were similar in lab- and vehicle-aged catalysts.

The model obtained for $NO_x$ conversion from the experimental design expresses a good correlation with the experimental data and can therefore be used to predict the effects of various poisons and poison interactions. Alkali metals, Na and K, were found to have the strongest negative effect on the $NO_x$ conversion. This effect was accompanied by a considerable decrease in total acidity, i.e., ammonia storage capacity. Further, Mg, P × K and P × Na also resulted in significant catalyst deactivation. The interactions of P with alkali resulted in a decreased poisoning effect compared to the alkali metals alone. Also, S and P, and to a smaller degree also the Na × S interaction, were found to result in a reduced poisoning effect. The decreased effect of alkali metals in the presence of P and S is ascribed to the formation of phosphates and sulphates, preventing the interaction of the alkali metals with the vanadia active sites. The effect of Zn was not significant in this study.

The surface areas of the contaminated catalyst samples were considerably decreased. However, no clear correlation between surface area and $NO_x$ conversion could be found. Also, no obvious correlation between the various contaminants and the surface area was observed, except for an indication towards decreased surface area from P and Mg contamination.

## Acknowledgements

The Swedish Energy Agency is gratefully acknowledged for financing this work within the FFI program Energy and Environment. Thanks also to Haldor Topsøe A/S for catalyst supply. Susanna Liljegren Bergman acknowledges partial support of the U.S. National Science Foundation (Grant CHE-1213216).

## References

[1] Regulation No 595/2009, Official Journal of the European Union, 18.7.2009 2009.
[2] O. Kröcher, M. Elsener, Appl. Catal. B 77 (2008) 215–227.
[3] E. Freund, A new process for the production of biodiesel by transesterification of vegetable oils with heterogeneous catalysis Sustainable Industrial Chemistry, Wiley-VCH, Weinheim, 2009, pp. 439–448.
[4] B.R. Moser, In Vitro Cell Dev. Biol.–Plant 45 (2009) 229–266.
[5] C.H. Bartholomew, Appl. Catal. A 212 (2001) 17–60.
[6] M. Klimczak, P. Kern, T. Heinzelmann, M. Lucas, P. Claus, Appl. Catal. B 95 (2010) 39–47.

[7] D. Nicosia, M. Elsener, O. Kröcher, P. Jansohn, Top. Catal. 42-43 (2007) 333–336.
[8] D. Nicosia, I. Czekaj, O. Kröcher, Appl. Catal. B 77 (2008) 228–236.
[9] G. Cavataio, H.-W. Jen, D.A., Dobson, J.R. Warner, SAE Paper 2009-01-2823.
[10] J.P. Chen, R.T. Yang, J. Catal. 125 (1990) 411–420.
[11] L. Chen, J. Li, M. Ge, Chem. Eng. J. 170 (2011) 531–537.
[12] J.P. Chen, M.A. Buzanowski, R.T. Yang, J.E. Cichanowicz, J. Air Waste Manag Assoc. 40 (1990) 1403–1409.
[13] H. Kamata, K. Takahashi, C.U.I. Odenbrand, J. Mol. Catal. A: Chem. 139 (1999) 189–198.
[14] Y. Peng, J. Li, W. Si, J. Luo, Y. Wang, J. Fu, X. Li, J. Crittenden, J. Hao, Appl. Catal. B 168–169 (2015) 195–202.
[15] F. Moradi, J. Brandin, M. Sohrabi, M. Faghihi, M. Sanati, Appl. Catal. B 46 (2003) 65–76.
[16] L. Lisi, G. Lasorella, S. Malloggi, G. Russo, Appl. Catal. B 50 (2004) 251–258.
[17] A.-C. Larsson, J. Einvall, M. Sanati, Aerosol Sci. Technol. 41 (2007) 369–379.
[18] A.-C. Larsson, J. Einvall, A. Andersson, M. Sanati, Top. Catal. 45 (2007) 149–152.
[19] A.-C. Larsson, J. Einvall, A. Andersson, M. Sanati, Energy Fuels 20 (2006) 1398–1405.
[20] Y. Zheng, A.D. Jensen, J.E. Johnsson, Ind. Eng. Chem. Res. 43 (2004) 941–947.
[21] Y. Zheng, A.D. Jensen, J.E. Johnsson, J.R. Thøgersen, Appl. Catal. B 83 (2008) 186–194.
[22] Å. Kling, C. Andersson, Å. Myringer, D. Eskilsson, S. Järås, Appl. Catal. B 69 (2007) 240–251.
[23] X. Guo, Poisoning and Sulfation on Vanadia SCR Catalyst, Department of Chemical Engineering, Brigham Young University, 2006.
[24] F. Castellino, S.B. Rasmussen, A.D. Jensen, J.E. Johnsson, R. Fehrmann, Appl. Catal. B 83 (2008) 110–122.
[25] H. Kamata, K. Takahashi, C.U.I. Odenbrand, Catal. Lett. 53 (1998) 65–71.
[26] Y. Xi, N.A. Ottinger, Z.G. Liu, Appl. Catal. B 160-161 (2014) 1–9.
[27] F. Castellino, A.D. Jensen, J.E. Johnsson, R. Fehrmann, Appl. Catal. B 86 (2009) 196–205.
[28] F. Castellino, A.D. Jensen, J.E. Johnsson, R. Fehrmann, Appl. Catal. B 86 (2009) 206–215.
[29] N.R. Draper, H. Smith, Appl. Regr. Anal., J. Wiley, New York, 1966.
[30] Y. Cheng, C. Lambert, D.H. Kim, J.H. Kwak, S.J. Cho, C.H.F. Peden, Catal. Today 151 (2010) 266–270.
[31] K. Wijayanti, S. Andonova, A. Kumar, J. Li, K. Kamasamudram, N.W. Currier, A. Yezerets, L. Olsson, Appl. Catal. B 166–167 (2015) 568–579.
[32] S. Shwan, J. Jansson, L. Olsson, M. Skoglundh, Appl. Catal. B 147 (2014) 111–123.
[33] S. Andonova, E. Vovk, J. Sjöblom, E. Ozensoy, L. Olsson, Appl. Catal. B 147 (2014) 251–263.
[34] J. Blanco, P. Avila, C. Barthelemy, A. Bahamonde, J.A. Odriozola, J.F.G. De La Banda, H. Heinemann, Appl. Catal. 55 (1989) 151–164.
[35] H. Jensen-Holm, N.-Y. Topsøe, J.J. Cui, Implementation of SCR DeNOx Technology on Coal-Fired Boilers in P.R. China, Lyngby, Denmark, 2006.
[36] N.-Y. Topsøe, Science 265 (1994) 1217–1219.
[37] N.Y. Topsøe, J.A. Dumesic, H. Topsøe, J. Catal. 151 (1995) 241–252.
[38] F. Castellino, Deactivation of SCR Catalysts by Additives, Department of Chemical and Biochemical Engineering Technical University of Denmark, Copenhagen, Denmark, 2008.
[39] N.-Y. Topsøe, J. Catal. 128 (1991) 499–511.
[40] M. Kleemann, M. Elsener, M. Koebel, A. Wokaun, Appl. Catal. B 27 (2000) 231–242.